JOURNAL OF APPLIED POLYMER SCIENCE VOL. 16, PP. 2317-2341 (1972)

The Plasma Polymerization of Vinyl Monomers. II. A Detailed Study of the Plasma Polymerization of Styrene

L. F. THOMPSON* AND K. G. MAYHAN, *Departments of Chemistry and Chemical Engineering and the Graduate Center for Materials Research, University of Missouri-Rolla, Rolla, Missouri 65401*

Synopsis

A study has been made on the plasma polymerization of styrene monomer in a cold, low-power, inductively coupled RF plasma. Styrene monomer yielded an insoluble, crosslinked film which was slightly colored. A kinetic study is reported for styrene. The effects of power level, bleed rate of monomer, pressure, and reactor geometry on the rate of polymer formation are reported. A mechanism is postulated for plasma polymerization. It was found that the initiation step was the rate controlling step and that the reaction followed a cationic polymerization scheme. Both crosslinking and discoloration of the polymers occur at the time of polymerization and are not a result of exposure of the reacted polymer to the plasma. The polymerization was shown to take place in the bulk phase as well as on the reaction wall surfaces.

INTRODUCTION

A series of nine monomers, which represented several generic classes, were studied and reported in part I of this series.[1] Styrene was selected for a comprehensive study of the reaction kinetics and a detailed chemical and physical evaluation of the products at various operating parameters. These detailed investigations and their results will be used to postulate a general mechanism for the polymerization of vinyl type monomers in a low-temperature RF plasma.

Initial experiments indicated that there were several parameters which affected the rate of plasma polymerization. The first of these parameters was the pressure in the reactor. There were three variables that could affect the operating pressure of the system. (1) Temperature: it was found that at the power levels used in these studies, the temperature remained constant over a time period which was longer than that for any single run, and hence the pressure was not affected. (2) Pumping speed: the pumping rate was a constant and a function of the physical size and location of the pump used (this did not fluctuate during any run). (3) Leaks: the virtual leak present in the vacuum system was a constant for

* Present address: Bell Telephone Laboratories, Murray Hill, New Jersey.

all of the experiments (the real leak rate was continuously variable from zero to 100 cc/min). This was the parameter which actually was used to control the pressure. For all of the kinetic experiments, a constant leak rate (0.061 g/hr) was used, and no inert gas was ever used in conjunction with the monomer.

The input power to the induction coil from the RF generator was found to affect the rate of polymerization. The power could be accurately adjusted, and at a given level the power was stable within $\pm 1/4$ watt. This was one of the parameters investigated in the kinetic study.

The concentration of monomer in the gas phase (pressure) also affected the rate of polymerization. This parameter was regulated by the leak valve and could be controlled to 3% on an absolute basis. The pressure (leak rate) was the same for all of the kinetic experiments.

A cold trap was used to collect unreacted monomer and in each kinetic experiment to determine the amount of unreacted monomer for each set of conditions. Using this technique, it was possible to obtain a complete material balance, i.e., monomer input, polymer formed, and unreacted monomer output. The polymer formed under each set of operating conditions was characterized and the results correlated with the kinetic experiments.

The experimental details for the kinetic experiments and a description of the system have been given in the first paper of this series.[1] The experimental procedures utilized in the characterization studies are usually well known and hence will not be presented in detail. Any special modification of a technique will be noted prior to the discussion of results.

RESULTS

Kinetics

The kinetic results for the plasma polymerization of styrene are given in Table I and are illustrated in Figure 1. The variables power level, time, and reactor position at a constant bleed rate of 0.06 g/hr were evaluated.

TABLE I
Rate of Polystyrene Formation and Per Cent Monomer Conversion at Various Power Levels

Power (watts)	dP/dt (g/hr)[a]	% Monomer conversion[b]
8	0.019	30–35
13	0.035	60–65
18[c]	0.047	—
22	0.053	80–85
28[c]	0.056	—
36	0.057	100

[a] dP/dt values represent an overall rate of formation of polymer over the entire reaction length and cannot be related to $dP/dt_{initial}$ or dP/dt_{max}.

[b] Based upon entire reactor length.

[c] One point determinations.

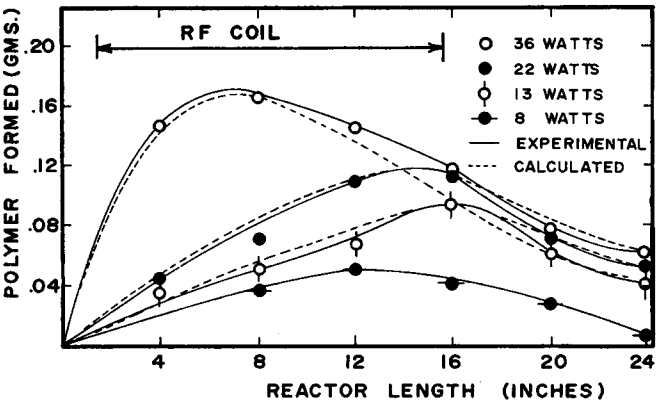

Fig. 1. Comparison of polymer formation for 12-hr runs compared to formation predicted by design equation.

Figure 1 shows that the mass of polymer formed increases as the power level increases at any point in the reactor and the position of the maximum rate of formation ($dP/dx = 0$) shifts inward toward the RF field as the power level increases. The 8-watt power level is the minimum required to sustain a plasma throughout the reactor length, and the data from these runs exhibit some anomalous behavior. The maximum rate of polymer formation would be expected to shift into the RF field since the density of active species at any point increases as the power density increases and this in turn results in an increased rate of polymerization.

When the data are plotted as a function of time, as shown in Figure 2, reasonable values of dP/dt for the entire reactor length can be obtained with power level as a parameter. These values are also presented in Table I along with the efficiency of monomer conversion. It can be seen that, for the particular experimental conditions employed here, prior to the power level of 36 watts the monomer was completely consumed before it traverses the length of the reactor. Figure 3 shows that for the present experimental

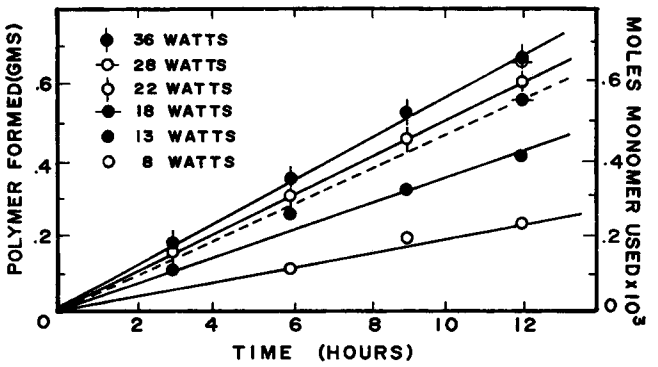

Fig. 2. Weight of polystyrene formed as a function of time.

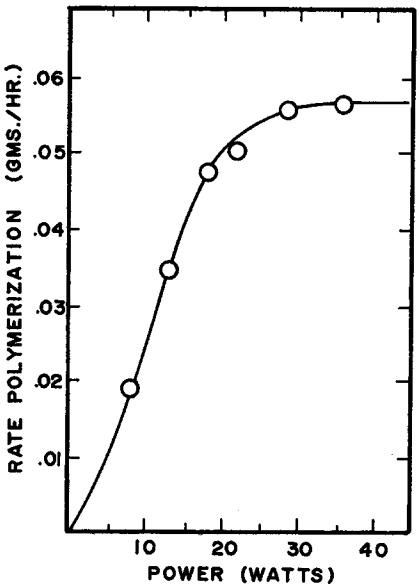

Fig. 3. Rate of polymer formation as a function of power.

parameters, the monomer was completely consumed at a power level of 28 watts. This number established the optimum power level and conditions for a reaction system of this design. A closer look at the data shows that the rate of polymer formation, 6–8 in. beyond the RF field, becomes insignificant with the geometry used in this study. The bleed rate of monomer into the system can be obtained from Figure 3 as a check on the calibration; 0.057 g/hr from the graph versus approximately 0.060 g/hr from the calibration data. The physical and chemical properties of polymer formed are dependent upon the power level and to a lesser extent upon reactor position.

The data presented in Figures 1 and 2 were also subjected to a routine kinetic interpretation. Figure 4 shows an Arrhenius-type plot of the data in the form

$$\ln \text{ (rate polymer formation)} = Ae^{-E_a/K'W}$$

where $-E_a$ is the apparent activation energy, W is the power input into the system in watts, and K' is a constant that includes time such that the product $K'W$ can be compared to the product RT from a standard Arrhenius expression. Since power input is the driving force for the polymerization reaction, this treament appears to be justified. The bulk temperature rises for the runs reported do not exceed 2°C over an ambient temperature of 25°C, and therefore the product RT has a value of about 600 cal/mole. If the rate data are then considered at specific time intervals, the value $K'W - KW_t$ can be compared to RT. A series of curves are generated, each

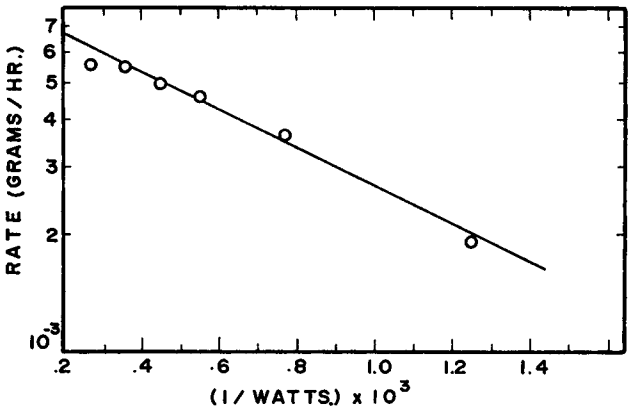

Fig. 4. Arrhenius-type plot of kinetic data.

of which has the same slope. By converting W_t to calories per mole, the product has the same units as RT and K is a dimensionless constant. Evaluation of K leads to a number in the range of $1\text{–}2 \times 10^{-5}$. This number has no quantitative value; however, qualitatively it can be stated that K is a very small number and that K' is a small number and therefore the activation energy for the polymerization is also small. Based upon the mechanism to be discussed later, it appears that the formation of an active species is the rate determining step for the reaction and that polymer formation is quite rapid.

Figure 4 also shows that the point for 36 watts falls off of the line. This reflects the previous statement that all of the monomer is consumed at this power level before it traverses the entire length of the reactor (these data are based upon total length). When only the RF field is considered, this point falls on the plotted line with no change in slope.

Characterization

The polystyrene that was produced by plasma polymerization consisted of two distinct phases, a soluble phase and an insolule phase. These phases were separated by solvent extraction methods and each portion analyzed by appropriate techniques. The purpose of these characterizations was to obtain enough information about the structure of the polymer in physical and chemical terms in order that a mechanism of polymer formation could be presented. The soluble polymer was present in very small quantities (usually less than 2%), and because of this limiting factor the types of characterizations were limited. The insoluble portion of the plasma polymerized polystyrene represented more than 98% of the total polymer formed and must be considered the major product. Molecular weight information could not be obtained on the insoluble material.

Infrared Spectroscopy

Infrared spectra were obtained for the soluble material using a Beckman IR-12. The sample was dissolved in methylene chloride and a film cast from solution of a KBr plate.

The spectrum of the soluble polystyrene produced in a 13-watt plasma is shown in Figure 5. The spectrum was obtained from a film deposited from a methylene chloride solution on a KBr plate. The spectrum is characteristic of a low molecular weight polystyrene and shows no anomalies.

The spectrum of the insoluble fraction of the above polymer was obtained using a KBr pellet and is shown in Figure 6. The low-resolution spectrum obtained for this sample is characteristic of a material that is not sufficiently ground to a fine enough powder so as to obtain high-resolution spectra. The nujol mull technique was also attempted; however, the results were not satisfactory. The spectrum is similar to a crosslinked polystyrene and indicates no anomalies or impurities.

Differential Thermal Analysis and Thermal Gravimetric Analysis

Differential thermal analysis (DTA) and thermal gravimetric analysis (TGA) were employed to study the thermal properties of the soluble and insoluble polystyrene using a Mettler thermal analyzer.

All of the samples were analyzed in both air and argon atmospheres in order that both oxidative and nonoxidative modes of thermal change could be studied. The results of the thermal analyses of the plasma-polymerized product were compared to two narrow molecular weight distribution linear polystyrene standards whose molecular weights were 20,000 and 1,000,000.

DTA–TGA traces were made on each soluble and insoluble polymer, provided enough material was available for testing. All of the results for the same type of polymer were essentially the same, and for this reason a typical result from the 22-watt study in argon will be used for discussion. Figures 7 and 8 show the general TGA traces for a soluble and insoluble polymer in comparison to a linear standard. The TGA results clearly show differences in the decomposition process of the soluble and insoluble polymers as a function of temperature and time. Figure 7 shows that the soluble polymer decomposes much more completely and much faster than the insoluble material. When the soluble materials are decomposed to a maximum temperature of 700°C in argon, no residue remains. When the insoluble polymer is treated in the same manner, a carbon network residue remains. The TGA curves for the insoluble polymer (Fig. 8) show that weight is lost at very low temperatures, <75°C, which is unexpected. The standard linear polystyrene, either the 20,000 or the 1,000,000 molecular weight, is stable until a few degrees before total decomposition occurs. These data indicate that the insoluble film contains some volatile components, perhaps monomer and dimer molecules, which were not removed during the solvent extraction. The insoluble films are more stable than the standard linear sample or the soluble polymers at high temperatures, and never was

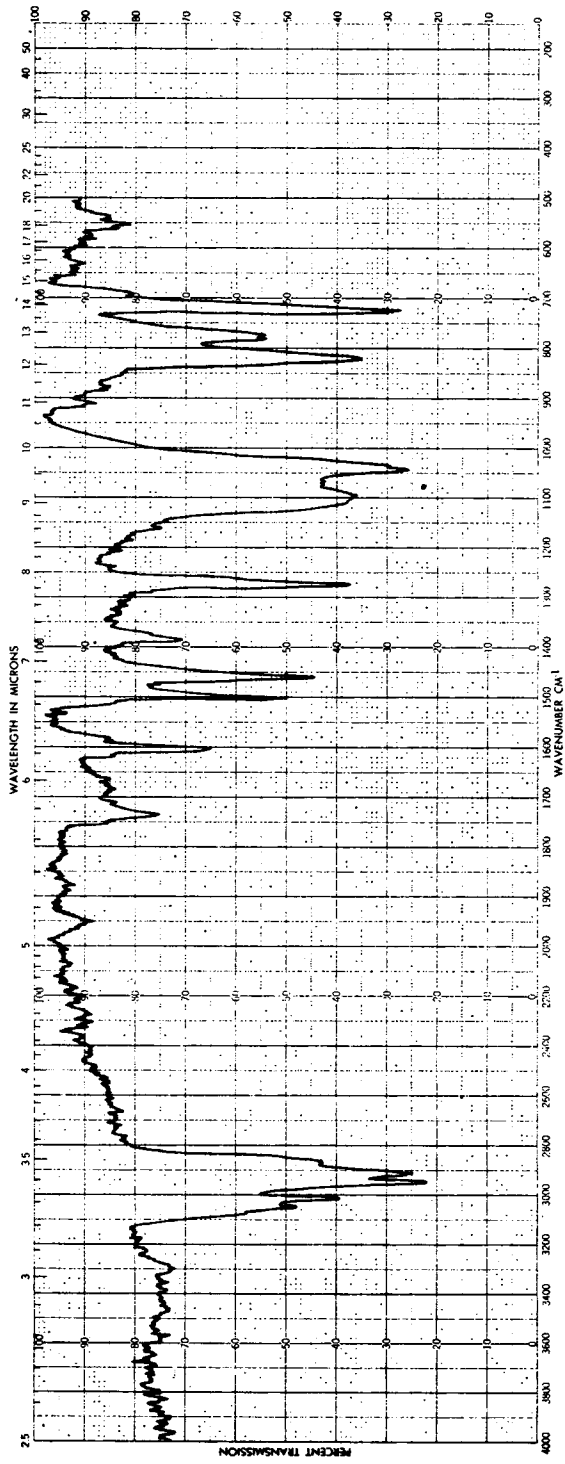

Fig. 5. Infrared spectrum of soluble polystyrene.

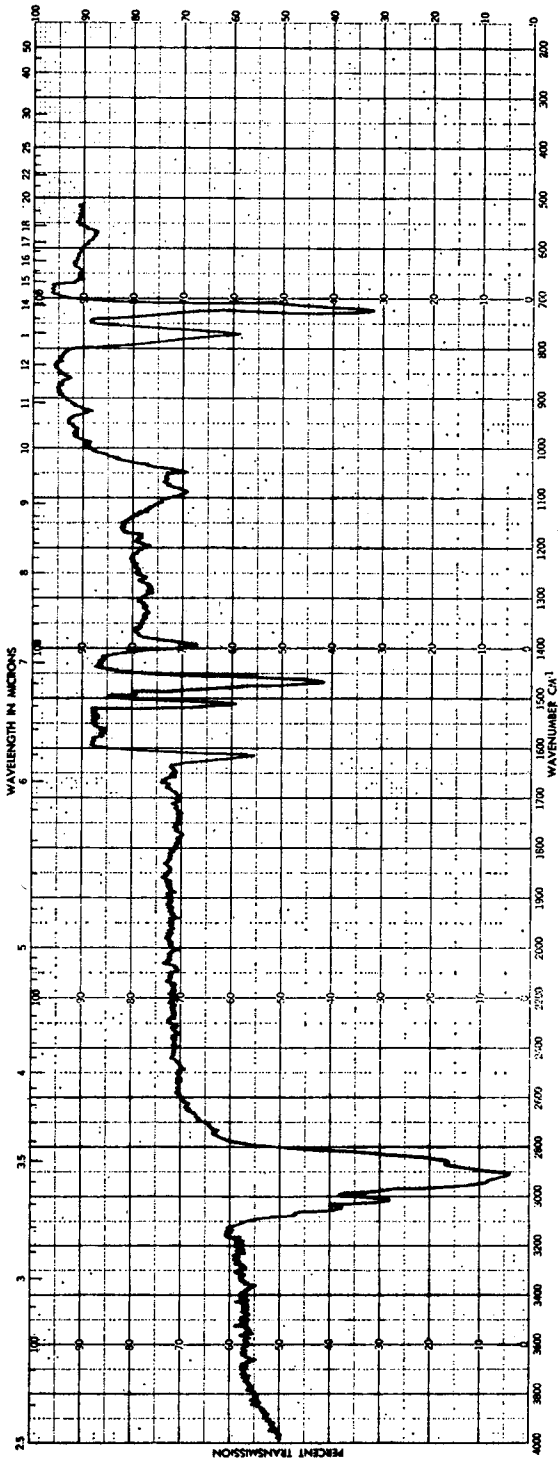

Fig. 6. Infrared spectrum of insoluble polystyrene.

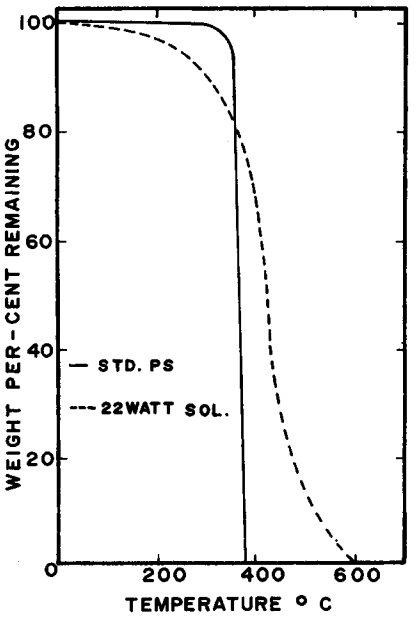

Fig. 7. TGA thermogram of soluble polystyrene from the 22-watt plasma polymerization.

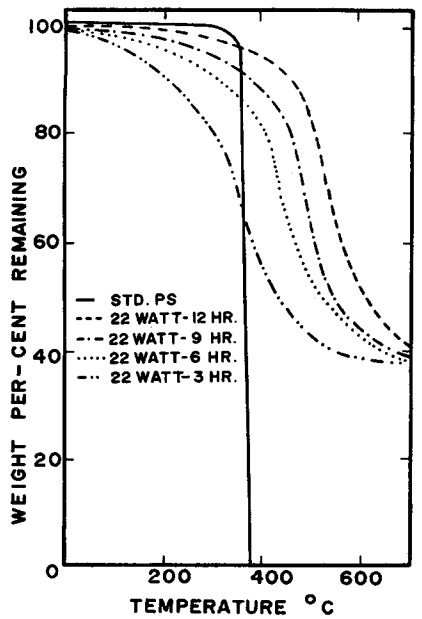

Fig. 8. TGA thermogram of insoluble polystyrene from the 22-watt plasma polymerization.

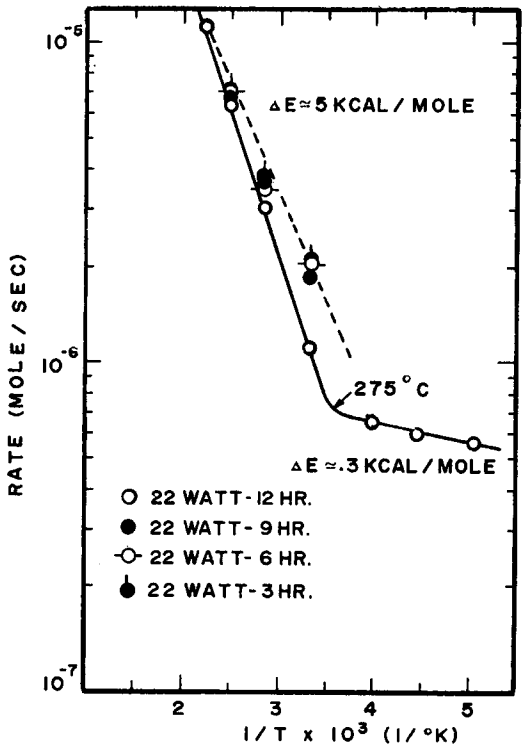

Fig. 9. Arrhenius-type plot from TGA data of the 22-watt plasma polymerization.

more than 60% of the initial weight lost from the insoluble sample over the temperature range 25°–700°C.

Weight loss data for the thermal decomposition of the insoluble polymer were obtained from the TGA traces of 22-watt runs as a function of both temperature and time. Figure 9 shows an Arrhenius plot for these data and indicates that weight loss from the polymer is occurring by different mechanisms below and above approximately 275°C. These processes exhibit different apparent activation energies, ~0.3 kcal/g-mole below 275°C and 4.0–5.0 kcal/g-mole above 275°C. The lower activation energy is interpreted as indication that small amounts of monomer or oligomers are evaporating from the surface of the polymer sample. Above 275°C, the polymer undergoes its first stages of decomposition. The 4.0–5.0 kcal/g-mole activation energy represents the net result of polymer decomposition products diffusing from within the bulk polymer particles and surface desorption. This activation energy is well within the normal range for low molecular weight species diffusing through a bulk polymer.[2]

The TGA results offer an indication of crosslinking. A carbon matrix remains from the insoluble polymer sample after the 700°C final temperature is achieved. This residue comprises about 40% by weight of the total initial sample weight and is not found in the soluble sample analysis or

analysis of the linear standards. This type of result would be expected from a crosslinked system and would account for the diffusion controlling loss in polymer weight. It is also consistent with the calculated activation energy of 5.0 kcal/g-mole. Figure 9 shows that the slope tends to decrease as the film thickness decreases (from 12 to 3 hr total polymerization time) and that the rate of weight loss correspondingly increases. This trend reflects changes in the polymer matrix due to decomposition as a function of film thickness. It should be noted that both the soluble and the linear polymers undergo a rapid decomposition and that the weight loss occurs entirely within a very narrow temperature range. Therefore, a treatment of the data under the conditions of these tests was not possible. Figure 8 also shows that the insoluble material that has been exposed to the plasma for the least amount of time loses weight faster in the low-temperature ($\leq$300°C) region. This indicates that volatile components are present in the matrix of the film since no decomposition is expected at these low temperatures.

The DTA results were the same for all of the insoluble samples. In air, two oxidation exotherms are observed, one at 320° ± 25°C and the other at 425° ± 25°C. The standard linear samples exhibit one sharp exotherm at the decomposition temperature of 350° ± 10°C. All of the argon analyses of the insoluble material indicated a broad exotherm occurring from the first point of decomposition until decomposition was complete. Below 275°C, little change in the base line for the DTA was noted, indicating no measurable endothermic or exothermic changes. Above 275°C a decomposition exotherm was evident in all cases. The magnitude of this exotherm for the standard linear and soluble polymers was considerably greater than was observed for the insoluble polymers.

Gel Permeation Chromatography

The molecular weights of the soluble polymers were obtained in toluene using a Waters Ana-prep gel permeation chromatograph. Gel permeation chromatography (GPC) was used to obtain two results for the soluble polymer. When employing careful recovery and dilution techniques, the area under the chromatogram peak gives an approximate quantitative value for the amount of soluble polymer recovered from each kinetic run. Molecular weights and molecular weight distributions were also obtained.

Semiquantitative results were obtained by comparing the area under the standard curves (2 ml of a 0.25% solution) with the area of the soluble polymer curve. These results indicate that the soluble polymer comprised less than 2% of the total polymer formed in all cases. For a given power level, the amount of soluble polymer increases with the reaction time; however, no mathematical correlation was found. The quantity of soluble polymer increases as the power level increases.

Figure 10 shows a typical GPC chromatogram obtained for the soluble polystyrene. The chromatogram indicates that a very low molecular

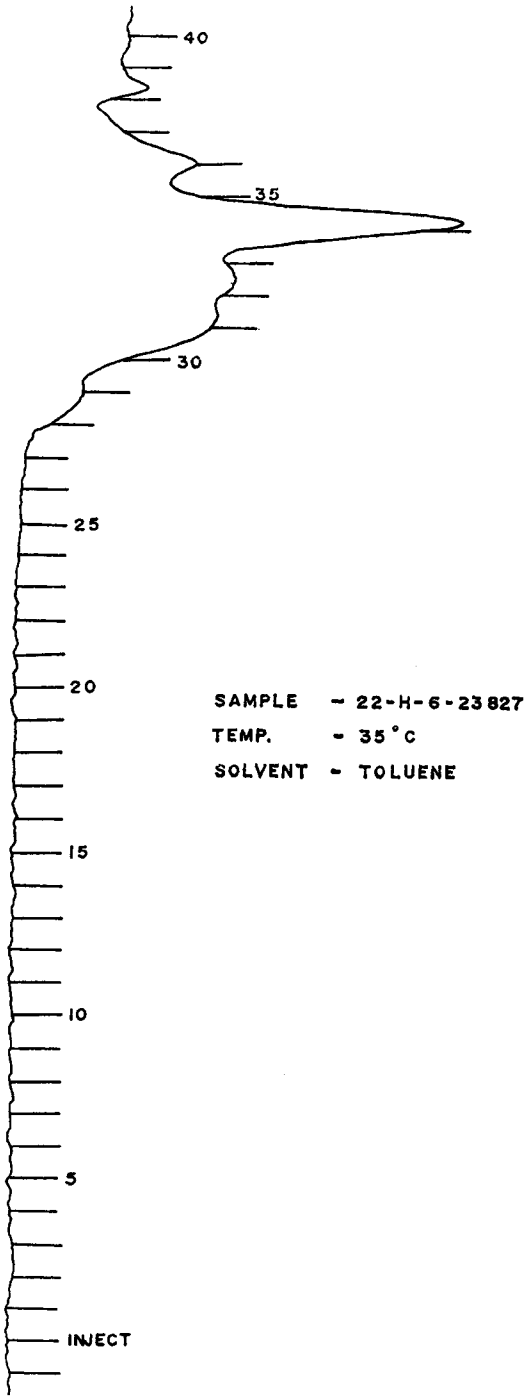

Fig. 10. GPC chromatogram of soluble polystyrene from the 22-watt plasma polymerization.

weight polymer was formed. Careful examination shows that the following elution marks correspond to the various x-mers of polymer: 36.8-monomer, 34.3-dimer, 32.5-trimer, 31.4-tetramer; above this, the molecular weights correspond to a high polymer. The chromatograms indicate that the soluble polymer consisted of very low molecular weight material and that the predominant species present were dimers, while trimers and tetramers comprised about 10% by weight of the total soluble polymer.

Mass Spectroscopy

Mass spectra were obtained for two samples using a Nuclide HT90 spectrometer. The two samples were a standard polystyrene sample of 20,000 molecular weight and the insoluble sample from the 22-watt 12-hr kinetic run. Tables II and III list the peaks in decreasing order of their relative intensities and the most probable species that give rise to each peak.

The most intense peak in both spectra corresponds to a mass to charge ratio of 91. This is to be expected as $C_7H_7^+$ will always form if at all possible since this carbonium ion is very stable. The major difference in the two spectra is that nearly all of the peaks from the linear polystyrene standard are some derivatives of either C_2H_x or C_4H_x. When the structure is examined, this is not surprising. The decomposition fragments are shown in parenthesis:

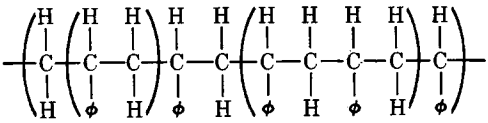

The spectra of the polystyrene from the 22-watt, 12-hr polymerization indicate that odd-carbon (C_3H_x,C_5H_x and C_7H_x) derivatives are the most

TABLE II
Mass Spectrometer Data for Standard Linear Polystyrene

M/e	Relative abundance	Contributing species
91	100	$C_7H_7^+$
104	92	$\phi C_2H_3^+$
30	44	$C_2H_6^+$
56	43	$C_4H_8^+$
27	33	$C_2H_3^+$
78	36	ϕCH^+
51	32	$C_4H_3^+$
103	29	$\phi C_2H_2^+$
55	27	$C_4H_7^+$
50	21	$C_4H_2^+$
77	13	ϕ^+
52	12	$C_4H_4^+$
57	9	$C_4H_9^+$
63	8	$C_5H_3^+$
65	7	$C_5H_5^+$
92	4	$C_7H_8^+$

TABLE III
Mass Spectrometer Data for Insoluble Polystyrene from 22 Watt 12 Hour Plasma Polymerization

M/e	Relative abundance	Contributing species
91	100	$C_7H_7^+$
39	64	$C_3H_3^+$
30	48	$C_2H_6^+$
77	44	ϕ^+
41	43	$C_3H_5^+$
78	34	ϕH^+
65	30	$C_5H_5^+$
114	27	$\phi C_2H_3^+$
63	25	$C_5H_3^+$
27	20	$C_2H_3^+$
67	16	$C_5H_7^+$
40	9	$C_3H_4^+$
105	7	$\phi C_2H_4^+$
54	7	$C_4H_6^+$
103	7	$\phi C_2H_2^+$
89	4	$C_7H_5^+$
115	3	$\phi C_2H_4^+$
53	2	$C_4H_5^+$

prevalent and the spectra are practically void of any C_2H_x or C_4H_x species. This would indicate that some structure anomaly is retarding the normal decomposition mechanism characteristic of linear polystyrene. One explanation of this would be that extensive crosslinking has occurred on the α-carbon in the polymer backbone as shown below.

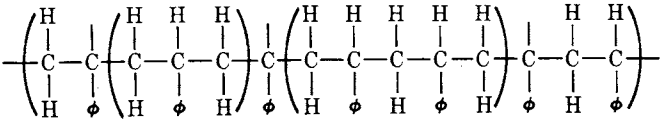

The decomposition occurs as a result of breaking carbon–carbon bonds. The carbons that were crosslinked have much less probability of fragmenting. By this mechanism, C_3H_x and C_7H_x would be expected to be the predominate linear fragments if the system was highly crosslinked.

X-Ray Analysis

A sample of insoluble polymer from each power level was investigated with x-ray techniques to determine if it contained short-range order that might contribute to the insolubility. The samples were ground to a very fine powder and stuck to a thin quartz filament that had been coated with petroleum jelly. The sample was then mounted and aligned in a Straumanis-type camera and exposed for 8 hr with a Seimans Crystalofles-4 x-ray unit. There was no indication of crystallinity in any of the polymers.

Scanning Electron Microscopy

Scanning electron microscopy (SEM) provided a useful technique for analysis of the polymer films formed in the plasma. Initially, the SEM technique was to be used to determine the homogeneity of the films. However, close examination of the product showed that solid spheres of polymer were embedded in the matrix of the polymer film. This phenomenon will be discussed in detail. A JSM-2 scanning electron microscope was used to obtain all of the micrographs. The micrographs from each power level will be discussed separately.

Figure 11 is a micrograph of the polymer produced by plasma polymerization at the 8-watt power level. The spheres shown are found in the film collected from the bottom of the reactor under the hot end of the RF coil. The surface sphere density is approximately 2.1×10^4 spheres per square inch as calculated from the micrographs. The spheres range in size from 0.2 to 1.7 microns in diameter, with an average diameter of 1.0 micron. Figure 12 is a micrograph of a single sphere. From this micrograph it is clear that the sphere is an individual particle which did not grow out of the film surface. Micrographs of films from the top of the reactor were completely void of spheres. As the sample is taken further downstream from the RF coil, the sphere density becomes less.

Figure 13 is a micrograph of the polymer produced at the 13-watt level. The sphere density for the 13-watt plasma-polymerized material is 2.7×10^5 spheres per square inch on the bottom of the reactor. The sphere size ranges from 0.5 to 1.0 micron, with an average size of 0.7 micron. The distribution is much more uniform in this sample. Polymers formed at the top of the reactor were free of spheres.

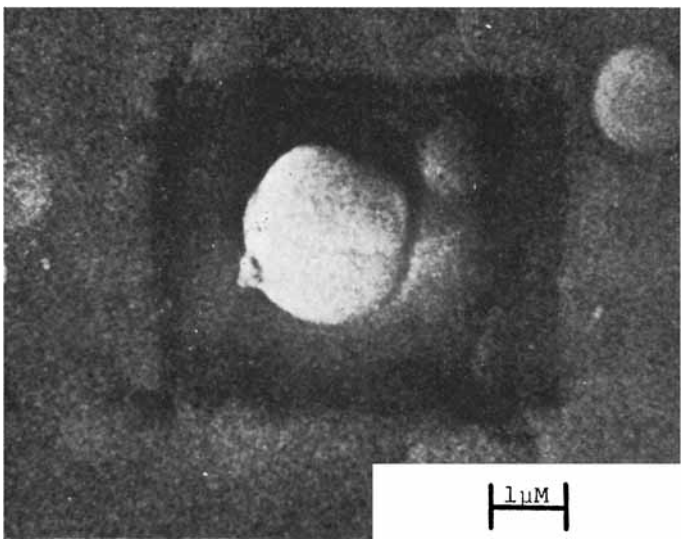

Fig. 11. Plasma polystyrene, 8 watts, 9 hr, sleeve 3, bottom of reactor.

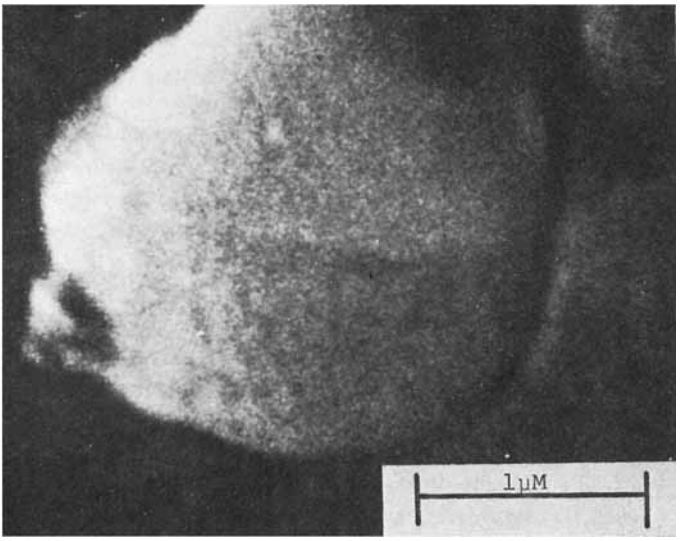

Fig. 12. Plasma polystyrene, 8 watts, 9 hr, sleeve 3, bottom of reactor.

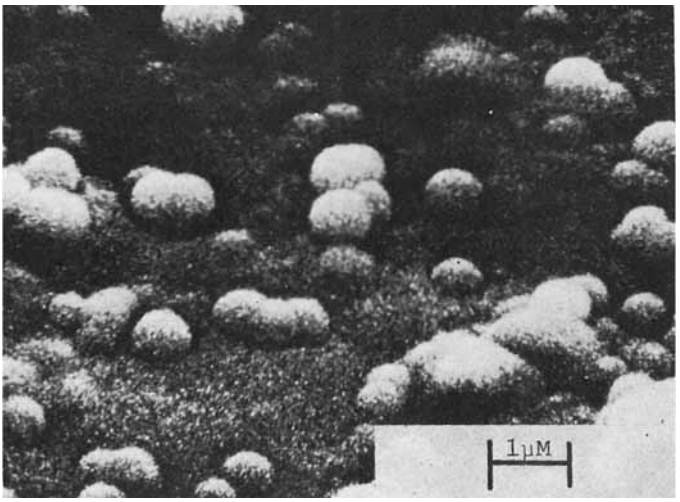

Fig. 13. Plasma polystyrene, 13 watts, 9 hr, sleeve 3, bottom of reactor.

Figure 14 is a micrograph of the polymer formed at the 22-watt power level. The sphere density is 3.9×10^5 spheres per square inch for the bottom of the reactor and their average size is 0.6 microns. The size distribution is small for this power level, with the diameters ranging from a minimum of 0.5 micron to a maximum of 0.7 micron. Figure 15 is a micrograph of the film from the top of the reactor and is free of spheres.

Figure 16 is a micrograph of the polymer from the 36-watt power level. The sphere density for this power level is 6×10^5 spheres per square inch.

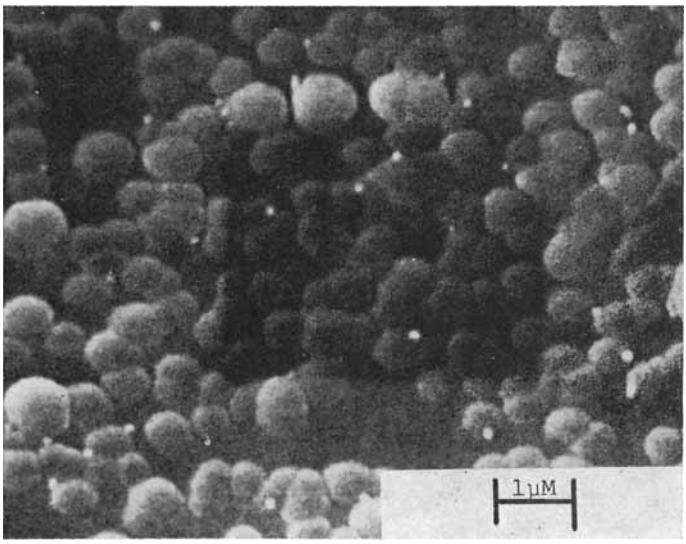

Fig. 14. Plasma polystyrene, 22 watts, 9 hr, sleeve 3, bottom of reactor.

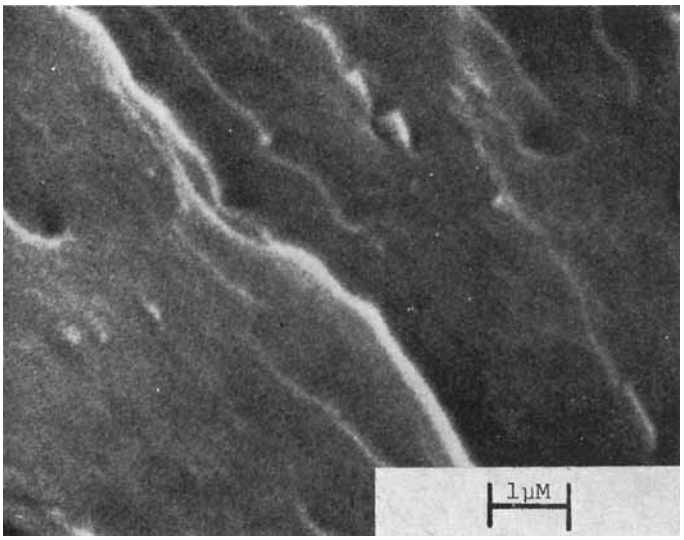

Fig. 15. Plasma polystyrene, 22 watts, 9 hr, sleeve 3, top of reactor.

The average size for the individual spheres is 0.5 microns, and the distribution is very narrow, with the sizes varying less than ±0.04 micron. Also at the 36-watt level the spheres comprise all of the polymer on the bottom of the reactor with no film matrix. While the reaction is in process at the 36-watt level the polymer is observed to form and fall to the bottom of the reactor in a manner reminiscent of a gently falling snow. The resulting spheres have been named "snow polymer."

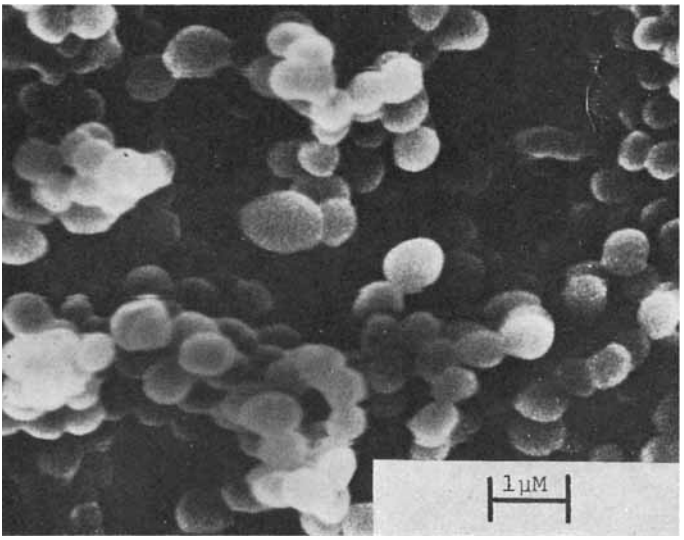

Fig. 16. Plasma polystyrene, 36 watts, 9 hr, sleeve 3, bottom of reactor.

From the micrographs discussed up to this point, three aspects should be emphasized. (1) The sphere density (density here refers to the number of spheres per unit area rather than a mass volume density) increases as the power is increased. (2) The spheres must be formed in the vapor phase of the reactor since no spheres are found on the top of the reactor, and hence they must be formed and then drop out of the gas phase onto the film in the lower half of the reactor. (3) The size of the spheres decrease as the power is increased. The distribution is also narrower at the high-power levels. This is consistent with the idea that the spheres are formed in the gas phase; and at the high power levels there are more sites to initiate sphere growth and the spheres are smaller because there is less monomer vapor around each growing sphere. Also, the spheres terminate faster because the plasma density is greater, as will be illustrated in the mechanism.

Figure 17 is a micrograph of a fractured edge of a film from the 13-watt plasma polymerization. The film was fractured in liquid nitrogen and mounted perpendicular to the electron beam. The micrograph shows that the spheres are embedded throughout the entire film and must form in the vapor phase.

Investigation of the Effect of a Plasma on Linear Polystyrene

The polystyrene formed through the plasma polymerization of styrene monomer is crosslinked and has a light-yellow to brown color. It is of interest to know if either of these properties were the direct result of being exposed to the plasma or if these properties were introduced at the time of polymer formation.

In order to determine the effect of the plasma on polystyrene, a film of standard linear polystyrene was exposed to the plasma. After 12 hr of

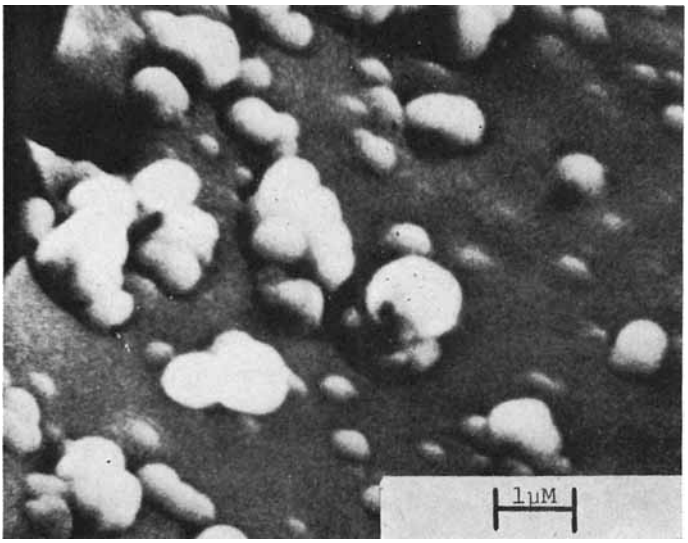

Fig. 17. Fractured edge of plasma polystyrene, 13 watts, 9 hr, sleeve 3, bottom of reactor.

exposure, the film showed no effect from the plasma. The solubility of the polymer was unaltered. The GPC chromatograms indicated the molecular weight was unchanged. The DTA thermograms and the IR spectra of the treated material were the same as those of the untreated standard. The color of the treated linear polystyrene did not undergo a noticeable change. These results indicate that the properties of insolubility and discoloration was introduced as the polymer network was formed. It can be concluded that the color observed in the plasma polymerization products resulted at the time of polymer formation and is most likely due to conjugation in the chains.

Investigation of the Initiation Step

In order to postulate a reasonable mechanism for the process and to have a sound idea of the fundamental chemistry involved in the plasma polymerization process, it was necessary to have some knowledge of the type of initiation that results in polymerization. There are three types of initiation steps possible: (1) free radical, (2) ionic, and (3) ion radical.

Two experiments were designed, one to detect the absence or presence of free radicals and the other, to detect the presence of ions.

The first experiment was designed to detect free radicals. Nitrogen dioxide is a very efficient free-radical scavenger, even in very low concentrations. If nitrogen dioxide is introduced into the system along with the monomer, the reaction should be retarded or inhibited if the initiation is occurring through a free-radical mechanism. The nitrogen dioxide will be excited by the plasma into ionic and free-radical species; however, the life of an ion of nitrogen dioxide is short at a pressure of 25 microns since re-

combination through wall collision is a predominant factor. This means that some of the nitrogen dioxide exists in its free state in the gas phase and should still serve as a scavenger species. With these possible limitations in mind, the following results were found.

Two concentrations of nitrogen dioxide were employed in two experiments; in one, a 10% by volume nitrogen dioxide and 90% by volume styrene monomer ratio was used, and in the other experiment, the concentration of scavenger (NO_2) was increased to 40%.

The scavenger gas did not affect the rate of polymerization in any measurable way. This would indicate that the initiation step is not occurring through either a free or an ion radical.

The second set of experiments was designed to detect the existence of ionic species in the plasma. The ion detection experiment employed a system which would electrostatically deflect a free ion traveling in the velocity stream of the plasma. Two gold electrodes were vapor deposited on a 20×6.8 cm glass tube. The resulting electrodes were 10×20 centimeters. The electrical connections were made by fixing two short pieces of copper grounding braid to the electrode surface with a silver conducting paste. The voltage leads were fed through two stopcocks using 12-gauge solid copper wire sealed in a $^{12}/_{5}$ standard ball joint with a low-vapor-pressure epoxy. The voltage was supplied from a 0–1850 V dc power supply designed to provide a pure dc signal with less than 0.5% ripple. When no voltage was applied to the plates, the plasma extended the entire length of the reactor. When voltages above 450 V dc were applied to the electrodes, a discharge plasma was initiated. This was undesirable since this introduced a different mechanism entirely. A voltage of 350 V dc was found to cause no dc plasma and was used for all of the deflection experiments. When the polymerization was initiated and the voltage applied to the electrodes, the plasma was stopped inside the electrode area. The greater part of the plasma was deflected toward the negative electrode, indicating that cations represented the geatest fraction of charged species. Experiments conducted at 22 watts for 12 hr showed that over 90% by weight of the polymer was deposited on the negative electrode and no polymer was formed downstream from the electrodes. The results of these experiments indicate the reaction is initiated through a cationic mechanism.

Mechanism

Plasma polymerization represents a unique method of carrying out a polymerization reaction. A mechanism is presented which is consistent with the experimental findngs. Each step in the mechanism will be discussed in terms of the preceding experimental data and by classical chemical concepts. Until now, mechanisms designed to explain plasma polymerization have involved surface adsorption as a primary step.[3–5] These investigators did not report any reaction occurring in the gas phase. Scanning electron micrograms clearly indicate that two mechanisms were occurring simultaneously: a surface reaction and a gas phase polymeriza-

tion. The surface reaction may follow some standard adsorption isotherm; however, it is clear that this type of interpretation is incomplete. The embedded spheres present in the film from the bottom of the reactor indicate that part of the reaction is occurring in the bulk gas phase. The mechanism presented here will not be discussed in terms of physical adsorption but rather in chemical terms. However, adsorption could occur at any point in the mechanism without destroying its validity. The mechanism will be discussed in four steps: (1) initiation, (2) propagation, (3) crosslinking and branching, and (4) termination.

1. Initiation. The initiation steps will be discussed as though ions or ion radicals could cause initiation, although the ion radical is less likely in light of the scavenger gas experiments. Molecules are excited in an RF plasma by elastic collision with accelerated electrons or accelerated ions. There are two possible chain of events that could result in an active monomer molecule. First the molecule may be converted to an excited state with no electrical charge, and then this excited molecule may fragment into active species capable of propagating polymerization. This series of steps may be represented as follows:

$$\mathrm{M} \xrightarrow{\Delta E} \mathrm{M}^* \tag{1}$$

$$\mathrm{M}^* + e \rightarrow \mathrm{M}^+ + 2e \tag{2}$$

$$\mathrm{M}^* + e \rightarrow \mathrm{M}^- \tag{3}$$

$$\mathrm{M}^* \rightarrow \mathrm{M}\cdot^+ + e \tag{4}$$

$$\mathrm{M}^* + e \rightarrow \mathrm{M}\cdot^- \tag{5}$$

$$\mathrm{M}^* \rightarrow \mathrm{P}^+ + \mathrm{Q}^- \tag{6}$$

where M = monomer molecule; ΔE = energy from plasma (this is manifested as an accelerated particle, usually an electron); M^* = excited monomer; M^- = anionic monomer molecule; M^+ = cationic monomer molecule; $\mathrm{M}\cdot^+$ = cation radical; $\mathrm{M}\cdot^-$ = anion radical; e = electron; and P^+, Q^- = styrene fragments.

Step (6) is of interest because both positive and negative charges are produced at the same time as the styrene monomer is fragmented. One example of this is as follows:

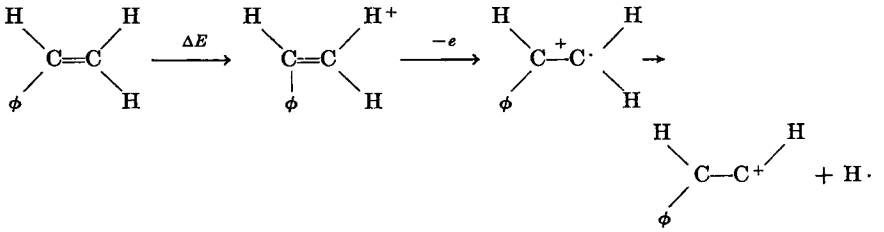

The second series of initiation steps are possible if the active monomer molecule capable of propagation is formed upon interaction with an ac-

celerated particle represented as in electrons. This possible series of steps is outlined below:

$$M + e \xrightarrow{\Delta E} M^+ + 2e \tag{7}$$

$$M + e \xrightarrow{\Delta E} M^- \tag{8}$$

$$M + e \xrightarrow{\Delta E} M\cdot^+ + 2e \tag{9}$$

$$M + e \xrightarrow{\Delta E} M\cdot^- \tag{10}$$

The formation of ions from collision with accelerated electrons in a plasma is analogous to the ionization that occurs in a mass spectrometer.[6] Free electrons are characteristic of all plasmas although the source of these electrons is not fully understood.

The remaining steps will be presented using the cationic monomer species, since from the deflection and scavenger gas experiments they have been shown to be the most abundant species. However, the presence of both ion radicals and anionic species has not been completely ruled out.

2. Propagation. The propagation steps outlined produced the long-chain polymer:

$$M^+ + M \rightarrow MM^+ \tag{11}$$

$$MM^+ + nM \rightarrow M(M)_aM^+ \tag{12}$$

3. Crosslinking and Branching. It has been shown in the foregoing sections that the insoluble polymer is most probably crosslinked. The x-ray diffraction patterns suggest that crystallinity is not responsible for the insolubility. Thus crosslinking is the most likely reason. The branching and crosslinking occur as a result of an active site being formed from interaction with the accelerated plasma particles. The following steps are postulated to account for the branching and crosslinking that have been shown to occur in the sample:

$$MMM(M)_nM^+ \xrightarrow{\Delta E} \underset{+}{M}MM(M)_nM^+ \tag{13}$$

$$\underset{+}{M}MM(M)_nM^+ + M \rightarrow \begin{matrix} M \\ M \\ M_+ \end{matrix}\!\!MM(M)_nM^+ \tag{14}$$

$$\begin{matrix} M \\ M_+ \end{matrix}\!\!MM(M)_nM^+ + nM \rightarrow \begin{matrix} M \\ M \\ (M)_n \\ M_+ \end{matrix}\!\!MM(M)_nM^+ \tag{15}$$

$$\begin{matrix} M \\ M \\ (M)_n \\ M_+ \end{matrix}\!\!MM(M)_nM^+ \xrightarrow{\Delta E} \begin{matrix} M \\ M^+ \\ (M)_n \\ M_+ \end{matrix}\!\!MM(M)_nM^+ \tag{16}$$

$$\begin{matrix} \mathrm{MMM(M)_nM^+} \\ \mathrm{M} \\ \mathrm{M^+} \\ \mathrm{(M)_n} \\ \mathrm{M_+} \end{matrix} + n\mathrm{M} \rightarrow \begin{matrix} \mathrm{MMM(M)_nM^+} \\ \mathrm{M} \\ \mathrm{M(M)_nM^+} \\ \mathrm{(M)_n} \\ \mathrm{M_+} \end{matrix} \tag{17}$$

$$\begin{matrix} \mathrm{MMM(M)_nM^+} \\ \mathrm{M} \\ \mathrm{MM(M)_nM^+} \\ \mathrm{(M)_n} \\ \mathrm{M_+} \end{matrix} \xrightarrow{\Delta E} \begin{matrix} \mathrm{MMM(M)_nM^+} \\ \mathrm{M} \\ \mathrm{{}^+MM(M)_nM^+} \\ \mathrm{(M)_n} \\ \mathrm{M_+} \end{matrix} \tag{18}$$

$$\begin{matrix} \mathrm{MMM(M)_n{}^+} \\ \mathrm{M} \\ \mathrm{{}^+MM(M)_nM^+} \\ \mathrm{(M)_n} \\ \mathrm{M} \\ \mathrm{M_+} \end{matrix} + \mathrm{nM} \rightarrow \begin{matrix} \mathrm{MMM(M)_nM^+} \\ \mathrm{M} \\ \mathrm{{}^+M(M)_nMMM(M)_nM^+} \\ \mathrm{(M)_n} \\ \mathrm{M} \\ \mathrm{M_+} \end{matrix} \tag{19}$$

The fact that some of the species have more than one charge on a single molecule is not impossible for a large molecule where the charges are separated by several carbon atoms. Furthermore, any of these charges could be terminated without affecting any of the other charges. Step (16) may appear to violate the expected chemical reaction as the α-hydrogen on a styrene is normally considered stable. However, hydrogen abstration is not unusual in a plasma, and active sites can be formed at any point along the chain.

Types of termination steps in a plasma may occur that are not possible with conventional techniques because there are excess negative charges present in the plasma. There are two facts to be recalled before the termination steps are presented. First, the soluble material has a very low molecular weight, which indicates that termination must occur quickly for some of the chains. This also means that crosslinking must be a predominant factor since no chain is allowed to grow to any appreciable length before it is crosslinked and rendered insoluble. Second, the product has a light-brown to yellow color, which indicates that unsaturation can occur as a result of ion pair rearrangement to form an unsaturated endgroup, see steps (20) and (22):

$$\mathrm{M(M)_nM^+} + e \rightarrow \mathrm{M(M)_nM} \tag{20}$$

$$\mathrm{M(M)_nC(H)(\phi)-C^+(H)(H)} + e \rightarrow \mathrm{MMC(H)(\phi)-C(H)(H)} \tag{21}$$

$$\mathrm{M(M)_nM^+} + \mathrm{C(H)(\phi)=C(H)(H)} \rightarrow \mathrm{M(M)_nC(H)(\phi)-C(H)(H)} + \mathrm{M^+} \tag{22}$$

$$\begin{matrix} \mathrm{MM(M)_nM^+} \\ \mathrm{M} \\ \mathrm{(M)_n} \\ \mathrm{M_+} \end{matrix} + 2\mathrm{e} \rightarrow \begin{matrix} \mathrm{MM(M)_n\overline{M}} \\ \mathrm{M} \\ \mathrm{(M)_n} \\ \mathrm{\overline{M}} \end{matrix} \tag{23}$$

$$\begin{matrix} MM(M)_nM^+ \\ M \\ (M)_n \\ M_+ \end{matrix} + 2M \rightarrow \begin{matrix} MM(M)_nM \\ M \\ (M)_n \\ M \end{matrix} + 2M^+ \quad (24)$$

$$\begin{matrix} MMM(M)_nM^+ \\ M \\ {}^+M(M)_nMMM(M)_nM^+ \\ (M)_n \\ M_+ \end{matrix} + 4e \rightarrow \begin{matrix} MMM(M)_nM \\ M \\ (M)_n \\ M(M)_nMMM(M)_nM \\ M \end{matrix} \quad (25)$$

$$\begin{matrix} MMM(M)_nM^+ \\ M \\ (M)_n \\ {}^+M(M)_nMMM(M)_nM^+ \\ M_+ \end{matrix} + 4M \rightarrow \begin{matrix} MMM(M)_nM \\ M \\ (M)_n \\ M(M)_nMMM(M)_nM \\ M \end{matrix} + 4M^+ \quad (26)$$

Steps (20), (21), and (22) will yield a soluble linear polymer. Branching with no crosslinking can occur if (23) and (24) or some modification of these reactions occur. Crosslinking seems to be the most pronounced effect and is terminated in a manner similar to (25) and (26). It is necessary to realize that on a molecule with more than one charge the termination may occur on only one charge permitting continued growth of the molecule. The plasma can also reinitiate a terminated molecule. These two ideas make extremely large molecules very likely.

CONCLUSIONS

As a result of this investigation, the following conclusions were drawn concerning the polymerization of styrene and other vinyl-type monomers in an inductively coupled RF low-temperature plasma:

1. Vinyl-type monomers can be converted to polymers in an inductively coupled RF plasma, utilizing either a horizontal or a vertical reactor assembly. The mass of polymer formed at any position in the reactor, under a specific set of experimental conditions, is dependent upon power level, bleed rate of monomer (a function of initial pressure), and time. At constant bleed rate and time, the amount of polymer formed increases as the power level increases. The efficiency of conversion of monomer to polymer, for a given reactor design, is dependent upon bleed rate and power level.

2. A routine kinetic treatment of the rate data fits an Arrhenius expression.

3. Gel permeation chromatographs showed that only about 1–2% of the plasma-formed polystyrene was soluble and that the soluble portion consisted of only oligomers.

4. Thermal analyses comparison of the plasma-formed polystyrene to a linear polystyrene indicated that the plasma polystyrene had a much greater stability than the linear polymer.

5. Mass spectra were obtained from the plasma polystyrene and a linear polystyrene standard. The fragmentation patterns seen to illustrate that the plasma-formed polymer was crosslinked to a high degree.

6. X-Ray patterns indicated that the plasma polysytrene did not possess any long-range order which could contribute to the insolubility of these polymers in organic solvents.

7. Scanning electron micrographs of the plasma polystyrene films showed clearly that the polymer formation is not solely an adsorption-controlled process. Polymer is also formed in the vapor phase.

8. A series of free-radical scavenger and ion deflection experiments showed that the polymerization proceeds through a cationic mechanism.

9. The crosslinking of the polystyrene occurs during the polymer formation.

10. A mechanism has been proposed which is consistent with the experimental findings of this investigation and which account for the physical and chemical properties of the plasma polystyrene.

References

1. L. E. Thompson and K. G. Mayhan, *J. Appl. Polym. Sci.*, **16**, 2291 (1972).
2. J. Crank and G. S. Park, *Diffusion in Polymers*, Academic Press, New York, 1968, pp. 74–255.
3. A. R. Denaro, P. A. Owens, and A. Crawshaw, *Eur. Polym. J.*, **4**, 93 (1968).
4. A. M. Mearns, *Thin. Solid Films*, **3**, 201 (1969).
5. T. Williams and M. W. Hayes, *Nature*, **209**, 769 (1966).

Received October 12, 1971
Revised April 7, 1972